

Frequency Diversity Measurements at 2.4 GHz for Wireless Sensor Networks Deployed in Tunnels

Ruoshui Liu
Computer Laboratory
Cambridge University
Cambridge, UK
Email: rl348@cam.ac.uk

Yan Wu
Computer Laboratory
Cambridge University
Cambridge, UK
Email: yw264@cam.ac.uk

Ian Wassell
Computer Laboratory
Cambridge University
Cambridge, UK
Email: ijw24@cam.ac.uk

Kenichi Soga
Department of Engineering
Cambridge University
Cambridge, UK
Email: ks207@cam.ac.uk

Abstract—Wireless Sensor Networks (WSNs) which utilise IEEE 802.15.4 technology operate primarily in the 2.4 GHz globally compatible ISM band. However, the wireless propagation channel in this crowded band is notoriously variable and unpredictable, and it has a significant impact on the coverage range and quality of the radio links between the wireless nodes. Therefore, the use of Frequency Diversity (FD) has potential to ameliorate this situation. In this paper, the possible benefits of using FD in a tunnel environment have been quantified by performing accurate propagation measurements using modified and calibrated off-the-shelf 802.15.4 based sensor nodes in the disused Aldwych underground railway tunnel. The objective of this investigation is to characterise the performance of FD in this confined environment. Cross correlation coefficients are calculated from samples of the received power on a number of frequency channels gathered during the field measurements. The low measured values of the cross correlation coefficients indicate that applying FD at 2.4 GHz will improve link performance in a WSN deployed in a tunnel. This finding closely matches results obtained by running a computational simulation of the tunnel radio propagation using a 2D Finite-Difference Time-Domain (FDTD) method.

I. INTRODUCTION

In recent years, Wireless Sensor Network (WSN) research has undergone a quiet revolution, providing a new paradigm for sensing and disseminating information from various environments using wireless technology. Currently, a multidisciplinary research group from the University of Cambridge is working on the application of WSNs for monitoring and assessing the condition of aged underground railway tunnels. In practice, the successful and effective deployment of WSNs is challenging owing to the harsh radio propagation environment that disrupts the radio communication links between wireless nodes owing to propagation path loss, channel fading and RF interference. These factors contribute to the dramatic variation in the received signal strength and consequently the variable bit error rate (BER) of the communication links. The question has been raised as to whether we can apply the Frequency Diversity (FD) technique to WSNs to combat signal fading and so improve the coverage and robustness of WSNs in the environments of interest.

FD has been studied in detail and implemented widely in cellular networks [1] in order to improve system BER performance and coverage. Lemieux in [2] and Todd in [3]

observed the improved performance due to FD in the indoor radio channels at 900 MHz and 1.75 GHz respectively for wireless personal communication. Generally speaking, FD has two main forms: Direct Sequence Spread Spectrum (DSSS) and Frequency Hopping (FH). The IEEE 802.15.4/ZigBee compliant RF transceiver [4] used in the Crossbow Technology Inc. MicaZ radio node employed in our experiments utilises DSSS. Furthermore, Dust Networks Inc. has incorporated FH in their proprietary Time Synchronised Mesh Protocol (TSMP) [5], but quantitative results concerning the performance benefits have not been presented.

Consequently, the potential benefits of applying FD needs to be quantified and characterised by performing accurate propagation measurements in the tunnel environment of interest. To do this in a realistic and inexpensive way we designed and built portable channel measurement equipment based on MicaZ nodes from Crossbow Technology Inc. In this paper, we present an analysis of the RF performance of the equipment in order to establish its suitability for this task. Specifically, we gained knowledge of the equipment transmit power and the Receive Signal Strength Indication (RSSI) characteristics over the system operating frequency range. The use of standard nodes will also permit us to take channel measurements in situations that closely replicate actual WSN deployments. The field measurements for tunnel wall mounted wireless sensor nodes have been conducted in the disused Aldwych London underground railway tunnel. The cross correlation coefficients of the fading data at various frequency channel spacings have been calculated using received signal power data gathered by scanning all the available channels in the unlicensed 2.4 GHz band. In addition, these results have been compared with those obtained from a simulation that uses the modified 2D FDTD method [6].

The paper is organised as follows. Section II introduces the design of the portable equipment for RF channel measurements, calibration of the equipment, measurement procedures and the geometry of the investigated tunnel. This is followed by the measurement results and analysis in Section III, and they are compared with the results from the simulation using 2D FDTD method. Finally, Section IV draws our conclusions and also proposes future work.

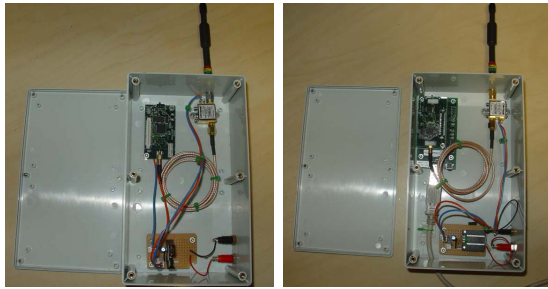


Fig. 1. Top views of the TxU on the left and the RxU on the right.

II. EXPERIMENTAL METHODOLOGY

A. Design of the Portable Equipment for RF Channel Measurements

The RF channel measurement equipment design is based around standard off-the-shelf Crossbow MicaZ motes [7]. The equipment consists of two subsystems, one acting as the Transmitter Unit (TxU) and the other one acting as the Receiver Unit (RxU). Fig. 1 shows views of the TxU and the RxU.

1) *The Transmitter Unit:* The TxU shown on the left in Fig. 1 has three main components: one Processor and Radio MPR2400CA board (top left), one power amplifier ZX60-2522M+ with a gain of 19.5 dB [8] (top right) and one Step-Down Integrated Switching Regulator (ISR) PT78ST133 [9] (bottom left). They are all housed in a plastic enclosure of dimensions 19.3 cm \times 11.3 cm \times 5.8 cm. The CC2420 RF transceiver is mounted on the MPR2400 board for the purpose of wireless communication. It is a single-chip 2.4 GHz IEEE 802.15.4 compliant RF transceiver designed for low power and low voltage wireless application. The MicaZ's CC2420 radio can be tuned from 2.048 to 3.072 GHz which includes the global ISM band at 2.4 GHz. IEEE 802.15.4 channels are numbered from 11 (2.405 GHz) to 26 (2.480 GHz) each separated by 5 MHz. The use of the transmitter power amplifier permits us to conduct extended range channel measurement campaigns in RF-hostile environments, such as tunnels.

2) *The Receiver Unit:* The CC2420 radio chip used in the Crossbow mote provides a very important piece of meta-data about received packets, specifically the Receive Signal Strength Indication (RSSI), which is a measurement of the received signal power in dBm. It is calculated over the first eight symbols after the start of a received packet. RSSI can also be measured at other times, for example to detect the ambient RF energy [10]. We use this feature to calibrate the receiver as will be described in Section II-B. The design of the RxU shown on the right in Fig. 1 is very similar to that of the TxU except it also has a mote interface board (MIB520) enabling RSSI data to be downloaded to a laptop PC. The four key components are: one Processor and Radio MPR2400CA board (top left), one MIB520 interface board on top of which the MPR2400CA board is attached, one low noise amplifier (LNA) ZX60-33LN+ [11] (top right) and one ISR 78SR105HC [12] (bottom). The LNA (ZX60-33LN+) has a gain of 13.5 dB and improves the

sensitivity of the receiver system by about 12 dB over that of the standard mote. The plastic enclosure for RxU has the same dimensions as that for TxU. The incorporation of the amplifier into the RxU further increases the channel measurement range and gives us greater freedom in the choice of measurement points.

B. Calibration of the TxU and the RxU

As has been identified in [13], in general, the off-the-shelf MicaZ motes that we have tested have a RF performance below the manufacturers' quoted specifications, and in addition, their characteristics vary from one to another. This is generally accepted owing to their relatively low cost and low power consumption. However, conducting measurements using uncalibrated motes is not to be recommended [14], [15]. Specifically, it is necessary to calibrate the TxU and the RxU before attempting the propagation measurements needed to quantify the availability of FD.

The mote variability can be overcome using the method proposed in [13] for calibrating pairs of motes using a networked computer driven instrument system. The method uses a MATLAB based computational environment running on a host PC to control a RF signal generator (SG), or a spectrum analyser (SA) depending whether the RxU or the TxU is being calibrated respectively in an unattended manner. These measures enable accurate estimation of channel path loss over the frequency band of interest to be performed.

1) *The RxU Calibration:* The calibration subsystem for the RxU is designed to eliminate the hardware dependency by creating an accurate mapping between the RSSI values and the actual received power at the RxU antenna connector for all 16 frequency channels. Fig. 2 shows one of the 16 (actually channel 11) lookup tables after the calibration process and processing.

2) *The TxU Calibration:* The calibration subsystem for the TxU is used to establish a lookup table for the transmit power from the TxU's RF connector as a function of frequency channel as shown in Fig. 3.

The outlined calibration process will considerably reduce errors owing to transmit power variation and RSSI variation as a function of frequency channel.

C. Experimental Set-up

Our FD measurements were conducted in the disused Aldwych underground railway tunnel in London. It is 3.76 m in diameter and 3.36 m from the track bed to the crown and has a cast iron lining. Dipoles made by European antennas (SVD2-2450-SMAF/951) with a gain of 2 dBi were used at the TxU and the RxU. These antennas are specified to operate over a frequency range from 2.40 to 2.50 GHz. The side mounted TxU was positioned on a pole 0.09 m away from wall A of the tunnel lining at a height of 2.20 m, and oriented vertically to the tunnel base as shown in Fig. 4. The use of a vertical antenna is to limit intrusion into the tunnel. The RxU was mounted on a pole at the same height as TxU.

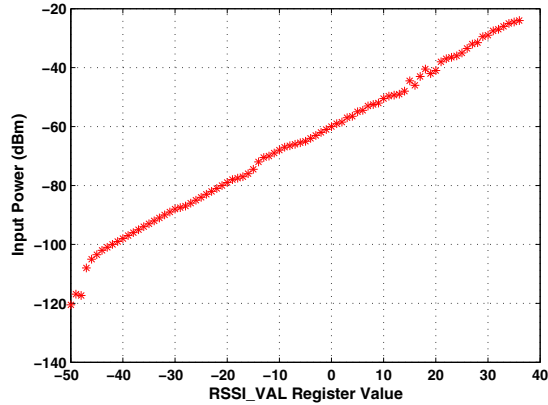


Fig. 2. Lookup table for the RxU under test after the processing for channel 11.

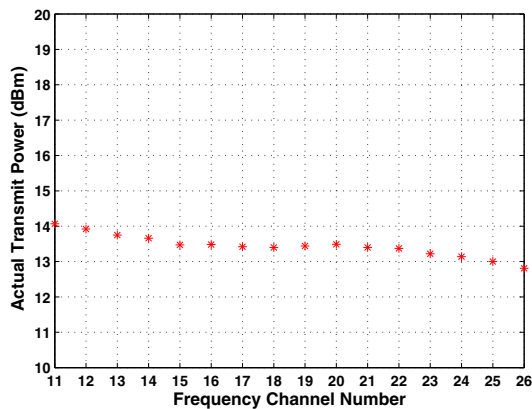


Fig. 3. Lookup table of the TxU under test across the 16 frequency channels.

To assess the availability of FD the TxU was programmed to hop through the 16 available frequency channels from 2.405 to 2.480 GHz, with a channel spacing of 5 MHz. The TxU/RxU were programmed to transmit/receive a packet every 0.25 s and to remain on each of the 16 radio channels for 1 s. The RxU recorded the received packets and their received signal power at varying distances from the TxU located on the same side of the tunnel as shown in Fig. 4. The RxU position varied between 10 m and 90 m in steps of 10 m and the RxU was stationary for 2 minutes while the data was gathered. Owing to limited access time to the tunnel, only Side to Same Side (S-SS) measurements were conducted.

III. FIELD MEASUREMENTS RESULTS AND ANALYSIS

FD is a technique to combat the fading phenomenon by transmitting information on more than one carrier frequency. By doing this, the hope is to find independent signal paths for communication so that if one radio channel undergoes a deep fade, i.e., high attenuation, another independent channel may have a strong signal, i.e., low attenuation [16]. So the propagation Path Loss (PL) represents the signal attenuation as a positive quantity measured in dB. To avoid confusion,

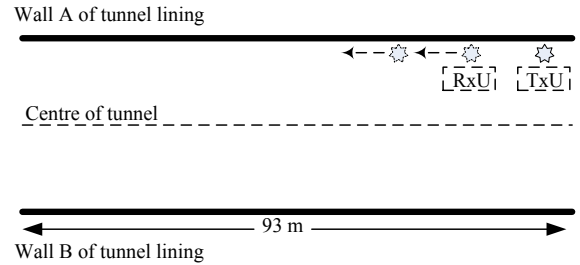


Fig. 4. Top view of the measurement geometry within Aldwych tunnel.

here we define the PL in dB as:

$$PL = P_{Tx} + G_{Tx} + G_{Rx} - P_{Rx} \quad (1)$$

where P_{Tx} is the transmit power at the TxU RF connector, P_{Rx} is the receive power at the RxU RF connector, G_{Tx} and G_{Rx} are the transmit and receive antenna gain respectively. P_{Tx} and P_{Rx} are obtained from the calibration tables established in Section II-B according to the operating frequency on which the data packets are transmitted.

A 3D plot of PL at an antenna separation of 30 m is shown in Fig. 5 where it can be seen that the PL for each of 16 frequency channels is generally constant with time owing to the limited amount of movement experienced in the tunnel. However, we note that some variation is evident in the measurements, e.g., about 10 dB on channel 19 (2.445 GHz) when the RxU is 10 m away from the TxU. In addition, variations of 5 dB are observed on channel 14 (2.420 GHz) and channel 21 (2.455 GHz) at locations of 10 m and 20 m respectively. These are believed to be owing to the fact that the other members of the team and underground staff were not stationary while measurements were taken.

The 3D plot in Fig. 5 also reveals that the mean value of the PL varies significantly from channel to channel giving rise to large variations in Signal-to-Noise Ratio (SNR) and hence Bit Error Rate (BER) on different channels at the RxU. The variation of PL between channels generally becomes smaller as the distance increases as can be observed from the standard deviation of the PL at each measurement location presented in Fig. 6. This suggests that the signals in different frequency channels will experience similar fading effects at longer range, i.e., they will be more highly correlated. Therefore, the benefit of applying FD at these ranges is likely to be less advantageous than at close range.

The success of the FD technique depends on the degree to which the signals on the different diversity branches are uncorrelated. Theoretically, frequencies separated by more than the coherence bandwidth of the channel will be uncorrelated and will thus not experience similar fading [2]. Calculations presented in [17] show that correlation coefficients as high as 0.7 are commonly used to define the coherence bandwidth. Note that greater gains are available from FD for smaller correlation coefficients. Analysis of the behaviour of the correlation coefficient as a function of the channel

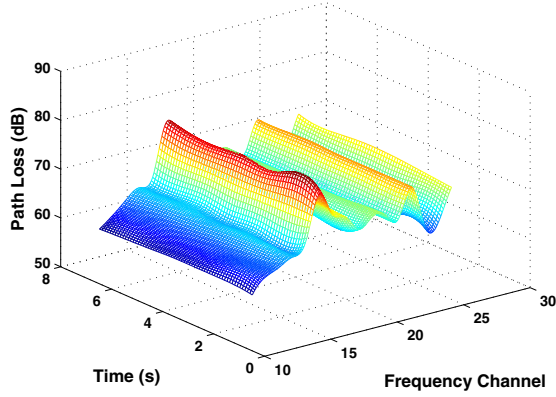


Fig. 5. Path loss on 16 frequency channels at 30 m.

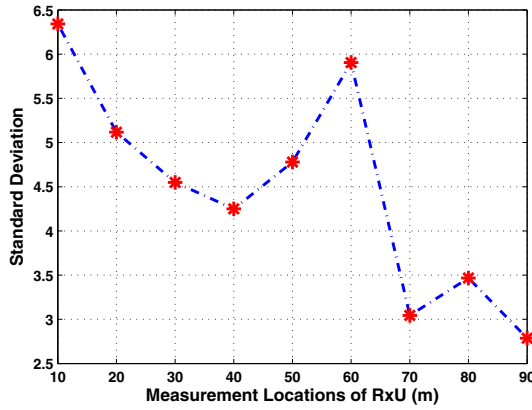


Fig. 6. Standard deviation of PL at different measurement locations.

(i.e., frequency) separation has been undertaken. The cross-correlation coefficient ρ between the two diversity channels is given in 2, and it is calculated by normalising the cross-correlation of the signals in the pairs of channels having the desired channel spacing,

$$\rho = \frac{\frac{1}{N} \sum_{n=1}^N x[n]y[n]}{\sqrt{\left(\frac{1}{N} \sum_{n=1}^N x[n]x[n]\right) \left(\frac{1}{N} \sum_{n=1}^N y[n]y[n]\right)}} \quad (2)$$

where $x[n]$ and $y[n]$ are the power gain sequences and N is the number of samples used in each sequence. The elements of each sequence are negated PL values in dB converted to a linear ratio. Note the power gain (which is <1) is used since it is directly proportional to the received power.

The availability of FD can be determined by computing the cross-correlation coefficient ρ between any two frequency channels with the same channel separation. For examples, the analysis of ρ for a channel separation of 1, i.e. 5 MHz, must be carried out by considering all the combinations of two channels with a channel separation of 1, e.g., channel 11 (2.405 MHz)

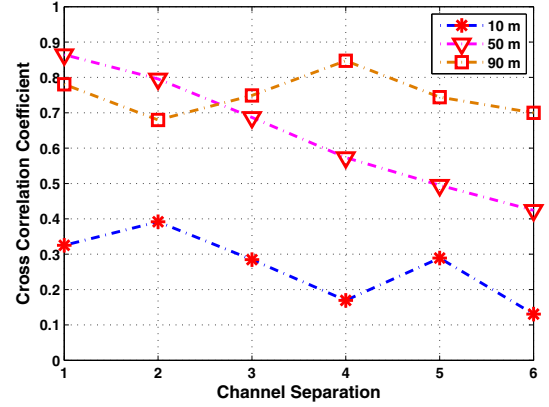


Fig. 7. Cross correlation coefficient obtained from measurements at 3 different locations: 10 m, 50 m and 90 m

and channel 12 (2.410 MHz), channel 12 and channel 13 etc. The 16 available radio channels in the ISM band permit ρ to be calculated up to the channel separation of 15. However, we observe that the number of different combinations of two channels with the same channel separation decreases as the channel separation increases. This will render the calculation of ρ statistically suspect owing to the decreasing number of samples present. Therefore, we only present the values of ρ up to a channel separation of 6. Fig. 7 show plots of ρ at 10 m, 50 m and 90 m.

From the short range (10 m) measurements presented in Fig. 7, in general, the values of the ρ decrease as a function of channel spacing and all lie well below the critical value of 0.7 implying that the application of FD will improve the communication performance. The decreasing trend in the value of ρ is also evident at 50 m. However, the magnitude of ρ shifts upwards compared with that at 10 m, even so, the values in general still remain below 0.7. At a separation of 90 m it can be seen that the cross-correlation coefficient does not exhibit the decreasing trend and is in general in excess of 0.7.

In general it can be seen that the cross-correlation values rise with increasing antenna separation. Further evidence concerning a reduction in variability across channels is given in Fig. 6 where it can be seen that the standard deviation decreases with antenna separation.

We have also conducted simulations using the modified 2D FDTD technique in order to investigate the cross-correlation coefficient for the tunnel of interest. Plots of the cross-correlation coefficient at 10 m, 50 m and 90 m based on simulation results are shown in Fig. 8. Generally speaking, the behavior of the cross-correlation coefficient computed based on simulation is consistent with those obtained based on field measurements. However, it can be seen that the value of ρ always lies below the critical value of 0.7. The declining trend in the cross-correlation coefficient as the channel separation increases is not evident at 90 m which is consistent with the measured results in Fig. 7. The reason why the magnitude of the cross-correlation coefficient at 90 m in the simulation (Fig.

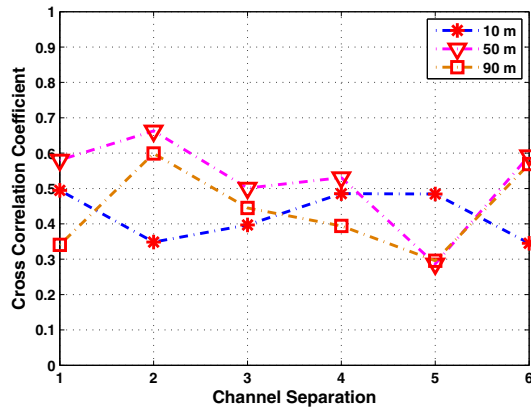


Fig. 8. Cross correlation coefficient after simulation at 3 different locations: 10 m, 50 m and 90 m

8) is generally smaller than those due to measurements (Fig. 7) is because the simulation assumes the tunnel lining material is a perfect conductor.

The calculation of ρ both from the field measurements and from simulations suggests that at close ranges a channel separation of 1, i.e. 5 MHz, at 2.4 GHz band is in excess of the coherence bandwidth, since the value of the cross-correlation coefficient lies well below 0.7. Therefore, a 5 MHz separation between the two channels is needed for the two signals to be substantially uncorrelated. Larger frequency channel separations generally yield lower values of cross-correlation coefficients implying that the frequency separation is much larger than the coherence bandwidth. However, at far range, the cross-correlation coefficient does not decrease with frequency and has a much larger magnitude than at close range. This implies that even widely separated frequency channels are still highly correlated and so FD will be less available for these scenarios.

IV. CONCLUSION

Received power measurements have been conducted at 16 frequency channels for the S-SS antenna positions in a tunnel in order to investigate and quantify the potential benefits of FD for WSNs in the 2.4 GHz band.

The cross-correlation coefficient between any two frequency channels having the same channel separation has been evaluated. The results obtained from the measurements and from the 2D FDTD simulations suggest two main findings. One is that the coherence bandwidth over which two frequencies of a signal are likely to experience correlated fading is less than 5 MHz at close range. Consequently it is worthwhile implementing FD in order to combat the channel fading effects. Also increasing the channel separation further reduces correlation. At far range, the benefit owing to the use of FD is likely to be reduced owing to greater correlation between the channels.

As part of our future work, we will perform measurements addressing the Centre to Centre and Side to Opposite Side

antenna cases in a tunnel environment.

ACKNOWLEDGEMENT

The authors would like to acknowledge the financial support of the Engineering and Physical Sciences Research Council (EPSRC) titled Smart Infrastructure: Wireless Sensor Network System for Condition Assessment and Monitoring of Infrastructure under Grant EP/D076870/1 and Japan Railway Technical Research Institute (RTRI).

REFERENCES

- [1] J. D. Gibson, *The mobile communications handbook*. IEEE press, 2000.
- [2] J. Lemieux, M. El-Tanany, and H. Hafez, "Experimental evaluation of space/frequency/polarization diversity in the indoor wireless channel," *IEEE Transactions on Vehicular Technology*, vol. 40, no. 3, pp. 569–574, 1991.
- [3] S. Todd, M. El-Tanany, and S. Mahmoud, "Space and frequency diversity measurements of the 1.7 GHz indoor radio channel using a four-branch receiver," *IEEE Transactions on Vehicular Technology*, vol. 41, no. 3, pp. 312–320, 1992.
- [4] A. Chipcon, "CC2420 2.4 GHz IEEE 802.15. 4/ZigBee-ready RF Transceiver," *Chipcon AS, Oslo, Norway*, vol. 4, 2004.
- [5] *Technical overview of time synchronized mesh protocol (TSMP)*, Dust Networks, Nov. 2008. [Online]. Available: <http://www.dustnetworks.com/technology/>
- [6] Y. Wu, M. Lin, and I. Wassell, "Modified 2D Finite-Difference Time-Domain Based Tunnel Path Loss Prediction for Wireless Sensor Network Applications," *Journal of Communications*, vol. 4, no. 4, p. 215, 2009.
- [7] C. Inc, "MICAz Datasheet." [Online]. Available: <http://www.xbow.com/>
- [8] Mini-Circuits, "ZX60-2522M+ Datasheet." [Online]. Available: <http://www.minicircuits.com/>
- [9] T. Inc, "PT78ST100 series datasheet." [Online]. Available: <http://www.ti.com/>
- [10] K. Srinivasan, P. Dutta, A. Tavakoli, and P. Levis, "Understanding the causes of packet delivery success and failure in dense wireless sensor networks," in *Proceedings of the 4th international conference on Embedded networked sensor systems*. ACM New York, NY, USA, 2006, pp. 419–420.
- [11] Mini-Circuits, "ZX60-33LN+ datasheet." [Online]. Available: <http://www.minicircuits.com/>
- [12] T. Inc, "78SR105HC datasheet," <http://pdf1.alldatasheet.com/datasheet-pdf/view/26762/TI/78SR105HC.html>.
- [13] R. Liu and I. J. Wassell, "A novel auto-calibration system for wireless sensor motes," University of Cambridge, Tech. Rep. UCAM-CL-TR-727, 2008.
- [14] S. Saha and P. Bajcsy, "System design issues for applications using wireless sensor networks," Automated Learning Group, National Centre for Supercomputing Applications, Tech. Rep. alg03, 2003.
- [15] Y. Yao and J. Gehrke, "The cougar approach to in-network query processing in sensor networks," *ACM Sigmod Record*, vol. 31, no. 3, pp. 9–18, 2002.
- [16] T. Rappaport, *Wireless communications: Principles and Practice*. Prentice Hall PTR Upper Saddle River, NJ, 2002.
- [17] W. Jakes, *Microwave mobile communications*. Wiley-IEEE Press, 1994.